Korean J. Chem. Eng., **25**(3), 431-436 (2008)

Preparation of Pt-Co catalysts on mesoporous carbon and effect of alloying on catalytic activity in oxygen electro-reduction

Ji Bong Joo, You Jung Kim, Wooyoung Kim, Nam Dong Kim, Pil Kim*, Younghun Kim, Youn-Woo Lee and Jongheop Yi†**

School of Chemical and Biological Engineering, Institute of Chemical Processes, Seoul National University, Shinlim-dong, Gwanak-gu, Seoul 151-744, Korea
*School of Environmental and Chemical Engineering, Chonbuk National University, Deokjin-dong 1ga, Deokjin-gu, Jeonju, Jeonbuk 561-756, Korea
**Department of Chemical Engineering, Kwangwoon University, Wolgye-dong, Nowon-gu, Seoul 139-701, Korea
(*Received 23 May 2007 • accepted 18 July 2007*)

Abstract−Mesoporous carbon (MC)-supported PtCo catalysts were prepared by a sodium borohydride ($NaBH_4$) reduction method. To increase the alloy degree of PtCo catalyst, the heat treatment was carried out at various temperatures (300-700 °C). The heat-treated PtCo catalysts (PtCo/MC-x) had the higher degrees of Pt-Co alloy than that of as-synthesized PtCo catalyst (PtCo/MC). MC supported-PtCo catalyst (PtCo/MC-500) that was treated at 500 °C, had the highest activity and lowest overpotential in oxygen electro-reduction (ORR) among the prepared PtCo catalysts. The high alloy degree and favorable chemical states of PtCo/MC-500 are believed to be responsible for the superior activity in oxygen electroreduction compared to the other PtCo catalysts.

Key words: Mesoporous Carbon, Electrocatalyst, PtCo, Oxygen Reduction, Fuel Cell

INTRODUCTION

Since mesoporous carbon CMK-x was first synthesized by Ryoo and co-workers, the mesoporous carbon materials have attracted tremendous attention due to their potential applications in the environment, electronics, electrochemistry and catalysis [1-6]. Mesoporous carbon materials have advantageous properties such as high surface area, high stability in extreme pH environment, and electro-conductivity. Because of its better physico-chemical and electro-properties, mesoporous carbon was successfully applied as the catalyst support in electrocatalysis [7-10]. Especially, considerable results have been reported for its use as a catalyst support in electrochemical reactions that occur in fuel cells [3,11-14].

Low temperature fuel cells have been considered as promising power sources for electronic devices and vehicles that require high energy density. Although considerable progress was achieved for performance improvement in the last decade [15-18], the high cost of Pt catalyst and low cathodic oxygen electroreduction activity have still remained as obstacles to overcome. The oxygen electroreduction reaction (ORR) is one of the most important reactions in oxygen-involving electroreactions such as metal-air batteries and fuel cells [19]. Because the ORR is kinetically slow, the development of highly active catalysts for ORR is essential. In the last decade, remarkable progress has been achieved in the fabrication of highly active Pt catalysts on cathodic oxygen reduction in low temperature fuel cells [20-23]. However, many obstacles such as the high cost of Pt electrode catalyst and the short lifetime of a low Pt-loading catalyst still remain for commercialization of fuel cells. It is necessary to design highly active Pt-transition metal alloy catalysts to reduce the cost and increase the performance and stability of fuel cells.

In this work, bimetallic PtCo catalysts on mesoporous carbon (MC) were prepared and alloy degree was controlled by post-preparation heat treatment. The prepared PtCo catalysts (PtCo/MC-x) were characterized by N_2-adsorption, TEM, XRD and electrochemical methods. The ORR activity was investigated by slow linear sweep method in an acidic electrolyte. In particular, the effect of heat treatment on the physicochemical properties and catalytic activity of MC-supported PtCo alloy catalysts was intensively investigated.

EXPERIMENTAL

1. Materials Preparation

Mesoporous carbon (MC) support was synthesized by typical templating method using mesoporous silica (MS) and sucrose as a templating material and a carbon, respectively. The detailed procedues are as follows. The aqueous sucrose solution containing diluted sulfuric acid was impregnated into the pores of the pre-prepared MS. The mixture was placed in a drying oven at 100 °C and subsequently dried at 160 °C for 6 h for sucrose polymerization. When the mixture turned dark brown, pyrolysis was carried out at 900 °C for 5 h under nitrogen gas. The resultant carbon-silica composite was treated with diluted HF solution to remove the silica template. The template-free carbon was filtered, washed with copious amounts of water and dried at 100 °C to give mesoporous carbon (MC).

Supported-PtCo catalysts were prepared by a sodium borohydride ($NaBH_4$) reduction method as described in the literature [24]. Pt precursor (H_2PtCl_6, Acrose) and Co precursor ($CoCl_2 \cdot 6H_2O$ Aldrich) were dissolved in deionized water and the carbon support MC

†To whom correspondence should be addressed.
E-mail: jyi@snu.ac.kr
‡This paper was presented at the 11th Korea-Japan Symposium on Catatysis held at Seoul, Korea, May 21-24, 2007.

was with an ultrasonicator. Aqueous 0.5 M $NaBH_4$ solution as reducing agent was added dropwise, and the mixture was kept at ambient conditions for 3 h under vigorous stirring to allow complete reduction of the metal precursors. The black precipitate was filtered and washed with copious amounts of water, and then MC-supported PtCo (PtCo/MC) catalyst was obtained. The metal content was maintained at 20 wt% in the catalyst, and the atomic ratio of Pt to Co was 3 : 1. To increase alloy degree between Pt and Co, heat treatment was carried out in a nitrogen atmosphere containing 10 vol% hydrogen at 300, 500 and 700 °C for 3 h. The heat-treated catalysts are designated as PtCo/MC-x, where x is the treatment temperature.

2. Characterization

Nitrogen adsorption isotherms of the prepared carbon support and catalysts were obtained by using a nitrogen sorptometer at 77 K (Micromeritics ASAP 2010). Pore size distributions were calculated by the BJH equation using the adsorption branch of the nitrogen isotherm. Small angle X-ray scattering (SAXS, GADDS Bruker) was used to investigate the crystallinity of mesostructured carbon on magnetite at 40 kV and 45 mA. The macroscopic morphologies and the metal dispersion of the prepared samples were observed by transmission electron microscopy (TEM, JEM-3010, Jeol). The X-ray diffraction (XRD) patterns of the prepared catalysts were recorded on an M18HF-SRA diffractometer (MAC Science) by using Cu-Kα radiation.

The electrochemical properties of the prepared catalysts were investigated with a conventional three-electrode system using a potentiostat (IVIUMSTAT, Ivium Technology). A saturated calomel electrode (SCE) and a platinum gauge were used as the reference electrode and the counter electrode, respectively. The working electrode was prepared by coating the catalyst ink on disk-type glassy carbon. The cyclic voltammetry technique was applied to investigate the electrochemical properties of the prepared catalysts. The cyclic voltammograms (CVs) were obtained at ambient temperature in 0.1 M $HClO_4$ solution between −0.25 and 1 V (vs. SCE) at 20 mV/s. The catalytic activities for the oxygen electro-reduction reaction (ORR) were evaluated by linear sweep voltammetry using a rotating glass carbon disk electrode (RDE 616, Princeton Applied Research). The linear sweep voltammograms of the prepared catalysts were recorded in oxygen-saturated 0.1 M $HClO_4$ solution in the range of 0.8 to 0 V (vs. SCE) at a scan rate of 5 mV/s at ambient temperature.

RESULTS AND DISCUSSION

The pore structures and pore size distributions of the MC support and the supported-PtCo catalysts were investigated by nitrogen adsorption. N_2 adsorption-desorption behavior, and the physical properties of the MC support and the supported-PtCo catalysts are shown in Fig. 1 and Table 1, respectively. MC support had irreversible type IV isotherms with well-developed hysteresis loop. PtCo/MC, PtCo/MC-300 and the PtCo/MC-500 had very similar N_2 adsorption isotherms. On the other hand, the N_2 adsorption isotherm of the PtCo/MC-700 was slightly different compared to that of MC support and the other PtCo catalysts. This is due to the partial deformation of the pore structure of the MC support caused by heat treatment and catalytic effect of supported PtCo nanoparticles, and

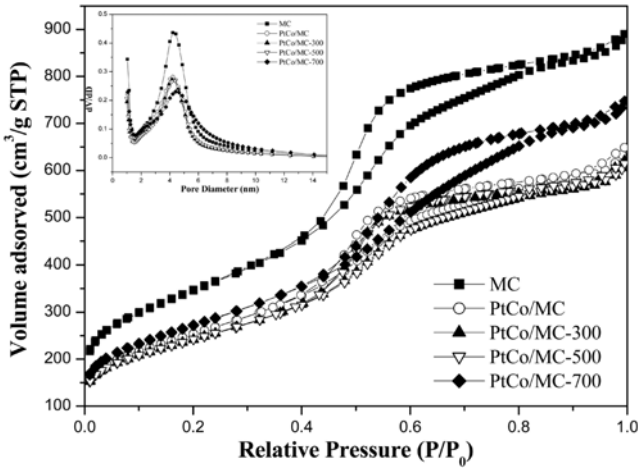

Fig. 1. Nitrogen adsorption isotherms and pore size distributions of the MC support and the prepared PtCo catalysts.

Table 1. Textual properties, average crystallite sizes calculated from the (220) diffraction plane using the Scherrer equation, surface areas of MC support and particle sizes from TEM analysis on the prepared PtCo catalysts

	Pore volume (cm^3/g)	S_{BET} (m^2/g)	D_{XRD} (nm)	S_{Pt} (m^2/g_{Pt})	D_{TEM} (nm)
MC	1.33	1229			
PtCo/MC	0.95	910	6.1	46	6.0
PtCo/MC-300	0.93	864	7.9	35	8.0
PtCo/MC-500	0.91	861	9.3	30	9.5
PtCo/MC-700	1.14	975	14	20	13.5

to partial collapses of cylindrical pores by metal sintering and during the heat treatment at 700 °C [25,26]. The MC support had a large surface area (above 1,200 m^2/g) and large pore volume (1.33 cm^3/g), while the supported PtCo/MC catalysts had smaller surface area and pore volume than MC support. Because of the metal content of PtCo in the prepared catalysts, the surface area and pore volume were about 0.8 times lower than that of the MC support. Among the prepared PtCo catalysts, the PtCo/MC-700 showed slightly higher pore volume and surface area.

Fig. 2 shows TEM images of the MC support and the MC-supported PtCo catalysts. A regular cylindrical pore structure was observed in the MC support (Fig. 2(a)). All of the PtCo catalysts show highly dispersed PtCo nanoparticles on the porous MC support. Among the supported PtCo catalysts, the PtCo/MC catalysts had the highest dispersion and the smallest PtCo nanoparticle size (Fig. 2(b)). As the heat treatment temperature increased, PtCo nanoparticles grew significantly. The metal sizes of PtCo/MC, PtCo/MC-300, PtCo/MC-500 and PtCo/MC-700 were about 6, 8, 9.5 and 13.5 nm, respectively. As seen in Fig. 2(e), the cylindrical pores of PtCo/MC-700 were partially broken. In small angle X-ray scattering (SAXS) patterns of PtCo/MC-700 (data not shown here), the small peak that is closely related to the orderness of the pore structure, was not observed. As mentioned in the N_2 adsorption experiment, these phenomena were caused by the deformation and partial collapse of the MC support pore structure by high-temperature heat treatment.

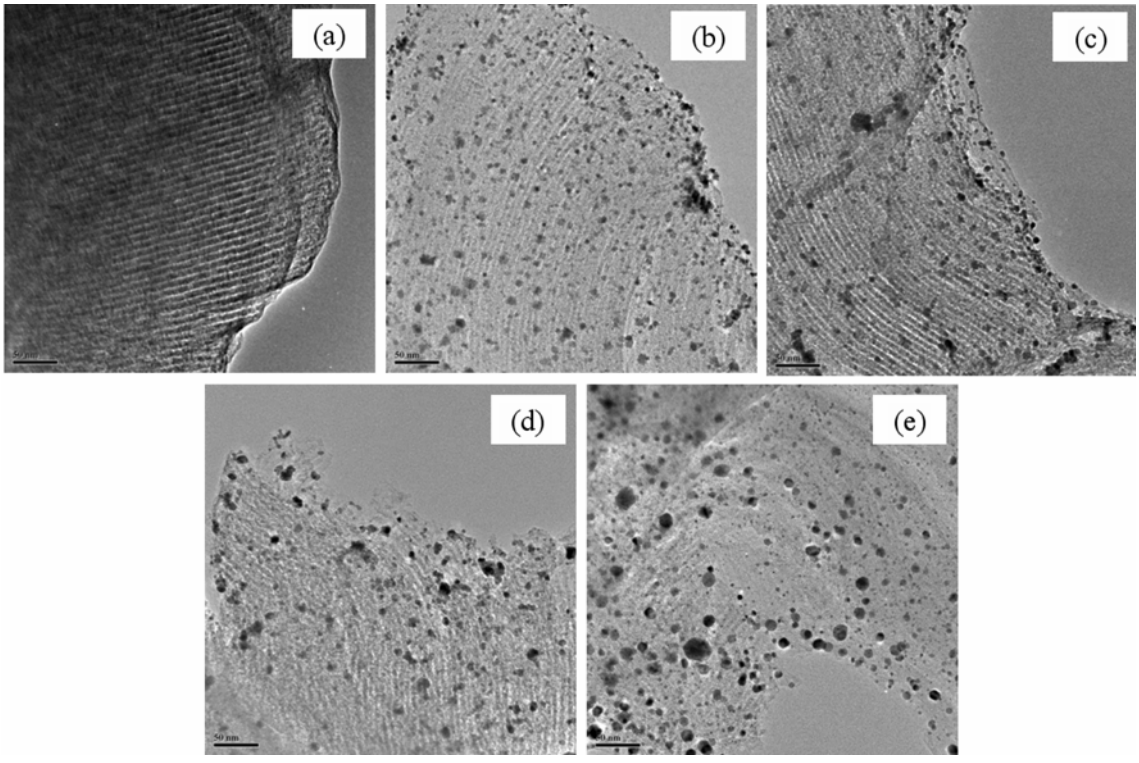

Fig. 2. TEM images of (a) MC support, (b) PtCo/MC, (c) PdCo/MC-300, (d) PtCo/MC-500 and (e) PtCo/MC-700 (Scale bar: 50 nm).

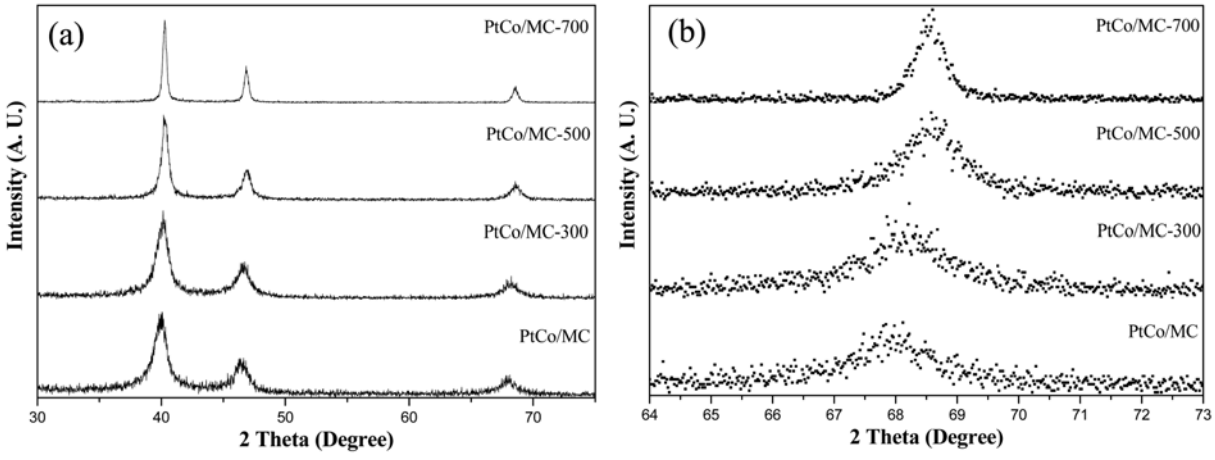

Fig. 3. (a) XRD patterns, (b) (220) peaks of the prepared PtCo catalysts.

The crystalline phases of MC-supported PtCo catalysts were identified by XRD. Fig. 3 shows XRD patterns of PtCo catalysts. No diffraction peaks related with Co species were observed. All PtCo catalysts showed typical characteristic peaks for (110), (200) and (220) which represent a faced-centered cubic (fcc) structure. In particular, the characteristic peaks for pure Pt (111) and (220) at 39.46° and 67.45°, respectively, shifted to the higher angles at 40.06° and 68.14°, respectively, for PtCo/MC. This angle shift is consistent with the formation of Pt-based alloy with another metal [27,28]. In particular, the (220) peak shift became more significant with heat treatment (Fig. 3(b)). Furthermore, the Pt (220) lattice parameters of the heat-treated PtCo/MC-x catalysts were smaller than that of PtCo/MC catalyst. The (220) lattice parameters of PtCo/MC, PtCo/MC-300, PtCo/MC-500 and PtCo/MC were 3.8886, 3.8786, 3.8667 and 3.8664, respectively. The Pt (220) lattice contracted significantly with treatment temperature. Heat treatment induced incorporation of the Co atom into the Pt lattice and the Pt-Pt distance decreased due to the small-sized Co atom. It is interesting to compare the degree of peak shift and lattice parameter of the PtCo catalysts, which can be considered to be an index of alloy degree. Thus, heat treatment significantly enhanced the alloy degree of PtCo/MC catalyst.

In addition, heat treatment would induce the formation of ordered Pt-M alloy crystalline phase. In case of PtCo alloy, the ordered Pt_3Co and PtCo type structures could be formed by the heat treatment, and the ordered PtCo crystalline structure has improved the catalytic activity in oxygen electro reduction [29-31]. In this study, the

prepared PtCo catalysts showed fcc structure peak only with small peak shift. Although ordered Pt_3Co and PtCo were reported to be thermodynamically stable [33], no ordered PtCo peaks were observed. This indicates that the prepared PtCo/MC-x catalysts are an alloy phase with the disordered crystalline structure. It is also reported that these disordered PtCo alloy catalysts showed higher ORR activity than pure Pt catalysts, and the alloy degree and activity were increased by heat treatment [34,35].

The diffraction peaks also became sharper with treatment temperature, indicating that the crystallite increased. The average crystalline size of PtCo nanoparticles was estimated according to the Scherrer formula based on the (220) plane. In addition, the surface areas of PtCo nanoparticles were calculated from Pt crystalline size using the following equation: $S=6000/\rho d$, where d is average crystallite size (nm), S is the surface area (m^2/g), and ρ represents Pt density (21.4 g/cm^3). The crystallite sizes and surface areas of Pt are listed in Table 1. The crystallite sizes for the PtCo catalysts are as follows: PtCo/MC<PtCo/MC-300<PtCo/MC-500<PtCo/MC-700. This trend is consistent with the estimates from TEM results.

The electrochemical properties were investigated by cyclic voltammetry in acidic electrolyte (0.1 M $HClO_4$). Fig. 4 shows the representative cyclic voltammograms (CV) of MC support and PtCo/MC-500 catalyst. The MC support showed large box-type CV indicating large electrochemical double layer capacitance (EDLC). Any H^+ ion adsorption-desorption, oxide formation and reduction current peaks were not observed. However, CV of PtCo/MC-500 showed a typical H^+ ion electro-adsorption region, a double-layer charging current region, a Pt pre-oxidation region and an oxygen reduction region. Results showed that MC support and MC-supported PtCo catalyst had high double-layer charging currents, which resulted from the high surface area of the MC support. Other MC-supported PtCo catalysts showed similar CVs compared to that of PtCo/MC-500. Generally, the peak area for the H^+ ion adsorption-desorption current is proportional to the electrochemically active surface area of Pt-based electrocatalysts. In the CV results, the order of H^+ ion adsorption peak current is: PtCo/MC>PtCo/MC-300>PtCo/MC-500>PtCo/MC-700. The electrochemically active surface areas (EAS) of PtCo/MC, PtCo/MC-300, PtCo/MC-500 and PtCo/MC-700 are 42, 32, 29 and 14 m^2/g_{Pt}, respectively. These results agree well with trends obtained from TEM and XRD analyses.

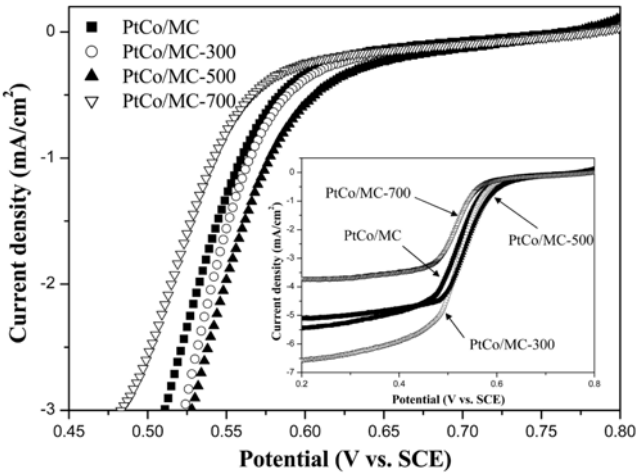

Fig. 5. Linear sweep voltammograms of the prepared PtCo catalysts and ORR polarization curves of the prepared catalysts in terms of onset potential in oxygen-saturated 0.1 M $HClO_4$ at a scan rate of 5 mV/s and a rotating speed of 1,600 rpm.

The linear sweep voltammetry technique was used to investigate ORR activity of the prepared catalysts by using a rotating disk electrode (RDE). Fig. 5 shows the ORR polarization curves and onset potential of MC-supported PtCo catalysts for oxygen electroreduction at 1,600 rpm in an oxygen-saturated 0.1 M $HClO_4$. From the polarization curves, the ORR is diffusion-controlled below 0.4 V and is mixed diffusion-kinetics-controlled in the potential range between 0.6 and 0.4 V. Because the metal content on the electrode was constant, the current density was closely related to mass activity (MA). Among the prepared PtCo catalysts, the PtCo/MC-500 exhibited the highest activity for the ORR in terms of onset potential and overpotential at a current density of 1 mA/cm^2. Because the oxygen reduction is kinetically slow, the onset potential and the current density in the Tafel region (between 0.6 and 0.8 V) are more important than the diffusion current density in the ORR experiments. In terms of onset potential and overpotential at a current density of 1 mA/cm^2, the order of ORR activity is as follows: PtCo/MC-500>

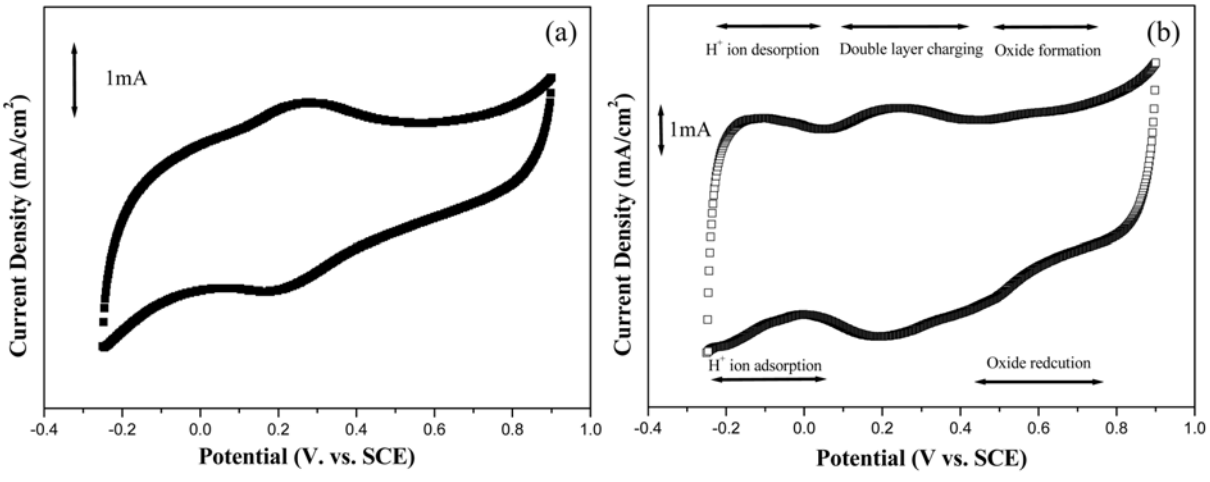

Fig. 4. Representative cyclic voltammograms of (a) MC support and (b) PtCo/MC-500 in 0.1 M $HClO_4$, at a scan rate of 20 mV/s.

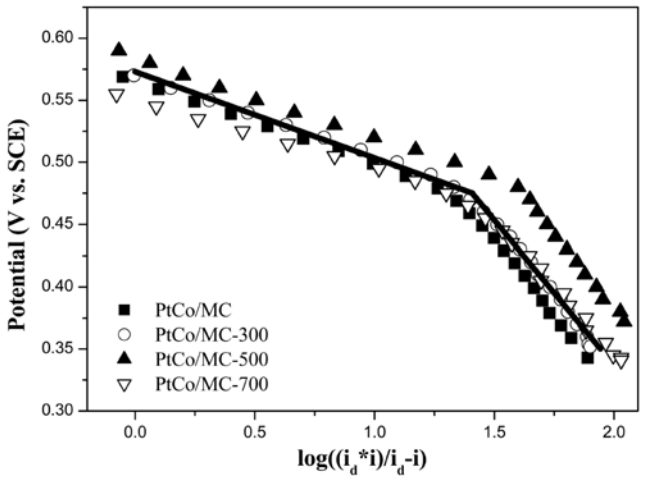

Fig. 6. Mass-transport-corrected Tafel plots for the oxygen reduction reaction of the prepared catalysts in oxygen-saturated 0.1 M $HClO_4$ saturated at a rotating speed of 1,600 rpm.

PtCo/MC-300>PtCo/MC>PtCo/MC-700. The highest ORR activity of PtCo/MC-500 can be ascribed to a high alloy degree between Pt and Co. Although the PtCo/MC-700 had the similar Pt lattice parameter and alloy degree compared to PtCo/MC-500, the particle size was significantly larger. The smallest PtCo surface area, caused by largest particle size, leads to low catalytic activity in oxygen electroreduction [33].

The electrocatalytic activities of the prepared PtCo catalysts for ORR were compared by Tafel plots. Fig. 6 shows mass-transport-corrected Tafel plots of the supported PtCo catalysts by plotting potential vs. $i \times i_d/(i_d - i)$, where i_d is the diffusion limiting current. In agreement with previous studies, all PtCo/MC catalysts have two different Tafel linear regions. In these two Tafel regions, all PtCo catalysts have similar Tafel slope values. This indicates that the ORR mechanism of the prepared PtCo catalysts was similar, as discussed in previous investigations [36-38]. These different Tafel slopes were explained in terms of coverage of oxygen adsorption with Temkin isotherm and Langmuir isotherm at low current density and high current density region, respectively. From the Tafel plots, the PtCo/MC-500 had the lowest overpotential indicating that it has the highest catalytic activity in oxygen electroreduction among the prepared PtCo catalysts.

The ORR activities of electrocatalysts are highly influenced by the chemical states of active metals such as lattice parameter, Pt-Pt interatomic distance and d-orbital vacancy [33-34]. Jalan and Taylor reported that ORR activities of carbon-supported Pt-based alloy catalysts were enhanced as a result of shortening the Pt-Pt interatomic distance by alloying Pt with another transition metal [39]. Appleby also claimed that lattice contractions due to alloying resulted in a more favorable structure for the dissociative adsorption of oxygen, while maintaining the favorable electronic properties [40]. Generally, as-synthesized carbon-supported Pt-based alloy catalysts have relatively low degree of alloy. Other post-process, such as heat treatment, could increase the alloy degree and develop ordered Pt alloy crystalline structure between Pt with other metals [27,28]. In our case, the chemical states of MC-supported PtCo, such as Pt lattice controlled by heat treatment. The contraction of the Pt lattice was closely related to the shortening of the Pt-Pt interatomic distance. Thus, PtCo/MC-500, which has small Pt lattice and high alloying degree, has the highest catalytic activity in oxygen electroreduction.

CONCLUSIONS

Mesoporous carbon-supported PtCo alloy catalysts were prepared by an $NaBH_4$ reduction method, and heat-treatment at various temperatures (300-700 °C) was carried out to investigate the changes in physicochemical properties and catalytic activity in oxygen electroreduction. Although the heat treatment at high temperature (700 °C) induced sintering of the PtCo active metal and deformation of mesoporous carbon support pore structure, the alloy degree of PtCo was significantly enhanced and favorable chemical states were formed at 500 °C. In oxygen electroreduction, the PtCo/MC-500 had the highest catalytic activity in terms of onset potential and the lowest overpotential in oxygen reduction among the prepared PtCo/MC catalysts. Based on these results, high catalytic activity is closely related to the high alloy degree and chemical states of PtCo/MC-500 that result from the heat treatment.

ACKNOWLEDGMENTS

This work was supported by grant No. (R01-2006-000-10239-0) from the Basic Research Program of the Korea Science & Engineering Foundation. J. Yi is grateful for an SBS Foundation grant and wishes to thank R. N. Zare, Stanford University, for his hospitality while this manuscript was prepared during his sabbatical.

REFERENCES

1. S. Jun, S. H. Joo, R. Ryoo, M. Kruk, M. Jaroniec, Z. Liu, T. Ohsuna and O. Terasaki, *J. Am. Chem. Soc.*, **122**, 10712 (2000).
2. R. Ryoo, S. H. Joo and S. Jun, *J. Phys. Chem. B*, **103**, 7743 (1999).
3. S. H. Joo, S. J. Choi, I. Oh, J. Kwak, Z. Liu, O. Terasaki and R. Ryoo, *Nature*, **412**, 169 (2001).
4. J. S. Han, S. Kim, W. Cho, H. Park, J. Yoon and T. Hyeon, *Microporous. Mesoporous Mater.*, **58**, 131 (2003).
5. J. Lee, J. Kim and T. Hyeon, *Adv. Mater.*, **18**, 2073 (2006).
6. T. Kang, Y. Park, K. Choi, J. S. Lee and J. Yi, *J. Mater. Chem.*, **14**, 1043 (2004).
7. L. Calvillo, M. J. Lazaro, E. Garcia-Bordeje, R. Moliner, P. L. Cabot, I. Esparbe, E. Postor and J. J. Ouitana, *J. Power Source*, **169**, 59 (2007).
8. S. H. Joo, C. Park, D. J. You, S.-A. Lee, H. I. Lee, J. M. Kim, H. Chang and D. Seung, *Electrochim. Acta*, **52**, 1618 (2006).
9. J. Ding, K.-Y. Chan, J. Ren and F. Xiao, *Electrochim. Acta*, **50**, 3131 (2005).
10. J.-H. Nam, Y.-Y. Jang, Y.-U. Kwon and J.-D. Nam, *Electrochem. Comm.*, **6**, 737 (2004).
11. P. V. Samant, J. B. Fernandes, C. M. Rangel and J. L. Figueiredo, *Catal. Today*, **102-103**, 173 (2005).
12. J. Ding, K. Y. Chen, J. Ren and F. Xio, *Electrochim. Acta*, **50**, 3131 (2005).
13. F. Su, X. S. Zhao, Y. Wang and J. Y. Lee, *Micropor. Mesopor. Mater.*, **98**, 323 (2007).
14. W. Choi, S. Woo, M. Jeon, S. Sohn, M. Kim and H. Jeon, *Adv.*

Mater., **17**, 446 (2005).
15. T.-H. Yang, G. Park, P. Paugazhendhi, W.-Y. Lee and C. S. Kim, *Korean J. Chem. Eng*., **19**, 417 (2002).
16. S. Lee, D. Kim, S. Lee, S. T. Chung and H. Y. Ha, *Korean J. Chem. Eng.*, **22**, 406 (2005).
17. C. Park, S. J. Lee, S.-A. Lee and H. Lee, *Korean J. Chem. Eng*., **22**, 214 (2005).
18. W. Hawut, M. Hunson and K. Pruksathorn, *Korean J. Chem. Eng*., **23**, 255 (2006).
19. K. Kinoshita, *Electrochemical Oxygen Technology*, John Wiley & Sons Inc (1992).
20. L. Xiong, A. M. Kannan and A. Manthiram, *Electrochem. Comm*., **4**, 898 (2002).
21. J. R. C. Salgado, E. Antolini and E. R. Gonzalez, *J. Power Sources*, **138**, 56 (2004).
22. K. Hirochima, T. Asaoka, T. Noritake, Y. Ohya and Y. Morimoto, *Fuel Cells*, **2**, 31 (2002).
23. W. Li, W. Zhou, H. Li, Z. Zhou, B. Zhou, G. Sun and Q. Xin, *Electrochem. Acta*, **49**, 1045 (2004).
24. P. Kim, J. B. Joo, W. Kim, J. Kim, I. K. Song and J. Yi, *Catal. Lett*., **112**, 213 (2006).
25. V. G. Pol, M. Motiei, A. Gedanken, J. Calderon-Moreno and Y. Mastai, *Chem. Mater*., **15**, 1378 (2003).
26. A.-H. Lu, W.-C. Li, W.-L. Salabas, B. Splierhoff and F. Schuth, *Chem. Mater*., **18**, 2086 (2006).
27. S.-A. Lee, K.-W. Park, J.-H. Choi, B.-K. Kwon and Y. E. Sung, *J. Electrochem. Soc*., **149**, A1299 (2002).
28. P. Kim, H. Kim, J. B. Joo, W. Kim, I. K. Song and J. Yi, *J. Power Sources*, **145**, 139 (2005).
29. B. C. Beard and P. N. Ross, *J. Electrochem. Soc*., **137**, 3368 (1990).
30. L. Xiong and A. Manthiram, *J. Electrochem. Soc*., **152**, A697 (2005).
31. L. Xiong and A. Manthiram, *J. Mater. Chem*., **14**, 1454 (2004).
32. E. C. Damari, M. C. Cadeville, J. M. Sanches and J. L. Moran-Lopez, *Phys. Rev. Lett*., **55**, 1208 (1985).
33. T. Toda, H. Igarashi, H. Uchida and M. Watanabe, *J. Electrochem. Soc*., **146**, 3750 (1999).
34. T, Toda, H. Igarashi and M. Watanabe. *J. Electroanal. Chem*., **460**, 258 (1999).
35. L. Zhang, K. Lee and J. Zhang, *Electrochem Acta*, **52**, 3088 (2007).
36. E. Antolini, J. R. C. Salgado, L. G. R. A. Santos, G. Garcia, E. A. Ticianelli, E. Pastor and E. R. Gonzalez, *J. Appl. Electrochem*., **36**, 355 (2006).
37. D. B. Sepa, M.Vojnovic and A. Damjanovic, *Electrochim. Acta*, **26**, 781 (1981).
38. Q. Huang, H. Yang, Y. Tang, T. Lu and D. L. Akins, *Electrochem. Comm*., **8**, 1220 (2006).
39. V. Jalan and J. Taylor, *J. Electrochem. Soc*., **130**, 2299 (1983).
40. A. J. Appleby, *Energy*, **11**, 13 (1986).